Remodeling of the Intestinal Brush Border Underlies Adhesion and Virulence of an Enteric Pathogen

RESEARCH ARTICLE

Remodeling of the Intestinal Brush Border Underlies Adhesion and Virulence of an Enteric Pathogen

Xiaohui Zhou,[a,b,c,d] Ramiro H. Massol,[e,f,g] Fumihiko Nakamura,[h] Xiang Chen,[a,b*] Benjamin E. Gewurz,[a,b] Brigid M. Davis,[a,b,c] Wayne I. Lencer,[e,f,g] Matthew K. Waldor[a,b,c]

Division of Infectious Diseases, Brigham and Women's Hospital, Boston, Massachusetts, USA[a]; Department of Microbiology and Immunobiology, Harvard Medical School, Boston, Massachusetts, USA[b]; HHMI, Boston, Massachusetts, USA[c]; Department of Pathobiology and Veterinary Science, University of Connecticut, Storrs, Connecticut, USA[d]; Division of Gastroenterology, Boston Children's Hospital, Boston, Massachusetts, USA[e]; Department of Pediatrics, Harvard Medical School, Boston, Massachusetts, USA[f]; Harvard Digestive Diseases Center, Boston, Massachusetts, USA[g]; Translational Medicine Division, Department of Medicine, Brigham and Women's Hospital, Boston, Massachusetts, USA[h]

* Present address: Xiang Chen, Laboratory of Zoonosis, Yangzhou University, Yangzhou, China.

ABSTRACT **Intestinal colonization by *Vibrio parahaemolyticus*—the most common cause of seafood-borne bacterial enteritis worldwide—induces extensive disruption of intestinal microvilli. In orogastrically infected infant rabbits, reorganization of the apical brush border membrane includes effacement of some microvilli and marked elongation of others. All diarrhea, inflammation, and intestinal pathology associated with *V. parahaemolyticus* infection are dependent upon one of its type 3 secretion systems (T3SS2); however, translocated effectors that directly mediate brush border restructuring and bacterial adhesion are not known. Here, we demonstrate that the effector VopV is essential for *V. parahaemolyticus* intestinal colonization and therefore its pathogenicity, that it induces effacement of brush border microvilli, and that this effacement is required for adhesion of *V. parahaemolyticus* to enterocytes. VopV contains multiple functionally independent and mechanistically distinct domains through which it disrupts microvilli. We show that interaction between VopV and filamin, as well as VopV's previously noted interaction with actin, mediates enterocyte cytoskeletal reorganization. VopV's multipronged approach to epithelial restructuring, coupled with its impact on colonization, suggests that remodeling of the epithelial brush border is a critical step in pathogenesis.**

IMPORTANCE **Colonization of the small bowel by *Vibrio parahaemolyticus*, the most common bacterial agent of seafood-borne enteric disease, induces extensive structural changes in the intestinal epithelium. Here, we show that this diarrheal pathogen's colonization and virulence depend upon VopV, a bacterial protein that is transferred into host epithelial cells. VopV induces marked rearrangement of the apical epithelial cell membrane, including elimination of microvilli, by two means: through interaction with actin and through a previously unrecognized interaction with the actin-cross-linking protein filamin. VopV-mediated "effacement" of microvilli enables *V. parahaemolyticus* to adhere to host cells, although VopV may not directly mediate adhesion. VopV's effects on microvillus structure and bacterial adhesion likely account for its essential role in *V. parahaemolyticus* intestinal pathogenesis. Our findings suggest a new role for filamin in brush border maintenance and raise the possibility that microvillus effacement is a common strategy among enteric pathogens for enhancing adhesion to host cells.**

Received 14 July 2014 **Accepted** 17 July 2014 **Published** 19 August 2014

Citation Zhou X, Massol RH, Nakamura F, Chen X, Gewurz BE, Davis BM, Lencer WI, Waldor MK. 2014. Remodeling of the intestinal brush border underlies adhesion and virulence of an enteric pathogen. mBio 5(4):e01639-14. doi:10.1128/mBio.01639-14.

Editor Vanessa Sperandio, UT Southwestern Med Center Dallas

Address correspondence to Matthew K. Waldor, MWaldor@research.bwh.harvard.edu.

This article is a direct contribution from a Fellow of the American Academy of Microbiology.

The luminal intestinal surface consists of densely packed, microscopic, actin-filled projections of the epithelial cell membrane, termed microvilli. These fingerlike projections are often disrupted when the intestine is colonized by enteric pathogens that closely adhere to and/or invade host cells. For example, enterohemorrhagic (EHEC) and enteropathogenic (EPEC) *Escherichia coli* both obliterate microvilli (also known as effacement) as they form attaching and effacing (A/E) lesions. These lesions are characterized by "intimate" pathogen attachment and the formation of pedestals—new, actin-rich structures that form on the epithelial surface—each of which typically cups a single, tightly adherent bacterium (1). *Vibrio parahaemolyticus*, the most common cause of seafood-borne enteritis, also induces extensive modification of the structure of intestinal tissue, both at a gross scale (destruction of villus architecture) and at finer resolution (both effacement and elongation of microvilli) (2, 3).

Many Gram-negative enteric pathogens, including those mentioned above, rely upon a specialized secretion apparatus, termed a type 3 secretion system (T3SS), to alter intestinal morphology. T3SS are syringe-like molecular machines that enable bacteria to

inject (translocate) diverse proteins into host cells (4). These "effector" proteins are known to modulate a wide variety of host cell processes, and T3SS are essential for the virulence of numerous bacterial pathogens (5).

Pathogenic isolates of *V. parahaemolyticus* encode two T3SS, one on each chromosome (6). T3SS1, which is also present in nonpathogenic isolates of *V. parahaemolyticus*, has been linked to cytotoxicity against a variety of cultured cell lines (reviewed in reference 7); however, analyses of T3SS1-deficient strains in animal models of disease suggest that this apparatus does not play a significant role in induction of intestinal disease (2, 8, 9). In contrast, T3SS2, which is present in the genome of only a subset of (typically virulent) *V. parahaemolyticus* strains, is essential for pathogenesis in several animal models. Inactivation of T3SS2 prevents *V. parahaemolyticus* colonization of the intestines of infant rabbits and all of the associated signs of disease (e.g., diarrhea, inflammation, tissue destruction, and microvillus effacement and elongation), and it similarly reduces enterotoxicity (fluid accumulation) and tissue destruction in surgically ligated ileal loops from adult rabbits (2, 8, 9). However, despite the pivotal role of T3SS2 in disease, it is not known how this pathogen induces such marked alterations in host tissue integrity and structure. Very few of the known T3SS2 effectors make readily detectable contributions to disease, and none have been mechanistically linked to the remodeling of the enterocyte brush border (BB) (10–13). In infant rabbits, only the multifunctional effector VopZ, which inhibits activation of innate immune signaling pathways, is known to be required for colonization (11). In ligated ileal loops, an actin-binding and bundling effector, VopV, is also required for enterotoxicity and is associated with loss of villous architecture (13); however, the role of VopV in an orogastric model of infection and disease and the processes by which this actin-binding effector contributes to pathogenesis have not been defined.

Here, we have further investigated the activity of VopV, which we independently identified via analysis of T3SS2-dependent protein secretion (11), in orogastrically infected infant rabbits, in a cell culture model of the intestinal brush border, and in several assays of protein interactions. We found that VopV is essential for *V. parahaemolyticus* colonization as well as pathogenicity in infant rabbits. Strains lacking VopV fail to induce effacement or elongation of BB microvilli, both *in vivo* and in tissue culture models of infection. Additionally, our *in vitro* assays indicate that such VopV-mediated remodeling of the apical BB membrane is a necessary precursor to adhesion of *V. parahaemolyticus* to the brush border; however, once effacement occurs, adhesion is VopV independent, suggesting that adhesion is a multistage process. Unexpectedly, VopV can induce effacement by two distinct means: by interacting with actin or through a previously unrecognized interaction with the actin-cross-linking protein filamin. Our findings suggest a new role for filamin in brush border maintenance and raise the possibility that microvillus effacement is a common strategy among enteric pathogens for enhancing adhesion to host cells.

RESULTS AND DISCUSSION

The T3SS2 effector protein VopV is a 1,622-amino-acid (aa) protein that consists of an N-terminal secretion signal, a series of interspersed repeat sequences, and a short C-terminal domain (Fig. 1A). A subset of the repeat sequences ("1" in Fig. 1A) and the C terminus were reported to bind actin and to induce fluid accumulation independently in rabbit ligated ileal loops (13), but the significance of VopV in intestinal colonization and pathology in an intact functioning intestine was not assessed. We compared intestinal colonization and associated pathology for infant rabbits orogastrically inoculated with wild-type (wt) *V. parahaemolyticus*, a mutant lacking *vopV* (Δ*vopV* mutant), or mutants in which the N-terminal region of VopV (which contains its secretion signal) was either truncated at that point (VopVn mutant), followed by two repeat sequences (VopVnR mutant), or followed by the C-terminal domain (VopVnC mutant) (Fig. 1A). Deletion of *vopV* was associated with an ~1,000-fold reduction in intestinal colonization relative to the wt strain, minimal intestinal fluid accumulation, and no overt diarrhea (Fig. 1B and C). Scanning electron microscopy (SEM) images of intestinal tissue from rabbits infected with the Δ*vopV* mutant were indistinguishable from images of uninfected rabbits, in which only the highly uniform tips of microvilli were apparent (Fig. 1D). Additionally, inflammatory cell infiltration and sloughing of epithelial cells that typify *V. parahaemolyticus*-infected tissue (2) were not observed in tissue sections from rabbits infected with the *vopV* mutant (Fig. 1E and F). In contrast, rabbits infected with the VopVnR or VopVnC strains (but not the VopVn strain) were colonized to the same extent as those infected with wild-type *V. parahaemolyticus* and had equivalent intestinal fluid accumulation, diarrhea, inflammation, and pathological changes in intestinal tissue (Fig. 1B to F). In SEM analyses for the wt, VopVnR, and VopVnC strains, large *V. parahaemolyticus* microcolonies were visible on the intestinal surface, surrounded by and sometimes embedded within highly extended and distorted microvilli. Effacement of the intestinal BB was also apparent in SEM (Fig. 1D), as previously observed using transmission electron microscopy (TEM) (2). These observations indicate that VopV is essential for *V. parahaemolyticus* intestinal colonization and all associated pathology and that VopV contains functionally redundant regions (i.e., R and C) that mediate its effects.

To investigate how VopV promotes *V. parahaemolyticus* intestinal colonization and pathology, we infected 14-day terminally differentiated monolayers of Caco-2_{BBe} cells, which form a uniform, well-structured BB (14) with strains carrying wt *vopV* or the mutant alleles described above. For these experiments, all strains also lacked the key T3SS1 gene *vscN1*, in order to avoid the cytotoxicity associated with this secretion system. Strains encoding full-length VopV, VopVnC, or VopVnR all induced marked disruption of BB microvilli, including microvillus effacement and elongation similar to those observed in infected rabbits (Fig. 2A, left). In contrast, the BB of monolayers infected with *V. parahaemolyticus* strains lacking *vopV* or a functional T3SS2 (Δ*vscN2* mutant) did not show formation of extended microvilli; instead, the normal microvillus structure was preserved, although a slight reduction of microvillus density was evident (Fig. 2A). Thus, the infected Caco-2_{BBe} monolayers generally phenocopy findings from *in vivo* studies of infected infant rabbits, thereby validating the cell line as a model system for study of *V. parahaemolyticus* pathogenicity. Visual analyses and enumeration of adherent CFU revealed that the Δ*vopV* and Δ*vscN2* strains adhered with lower frequency (~80% less) to Caco-2_{BBe} monolayers than strains producing VopV, VopVnC, or VopVnR (Fig. 2A and B). Together, these observations suggest that VopV promotes *V. parahaemolyticus* intestinal colonization and virulence by enhancing the bacteria's capacity to adhere to lumenal surfaces of enterocytes, perhaps by inducing rearrangement of the BB membrane.

To test if *V. parahaemolyticus* adhesion requires alteration of

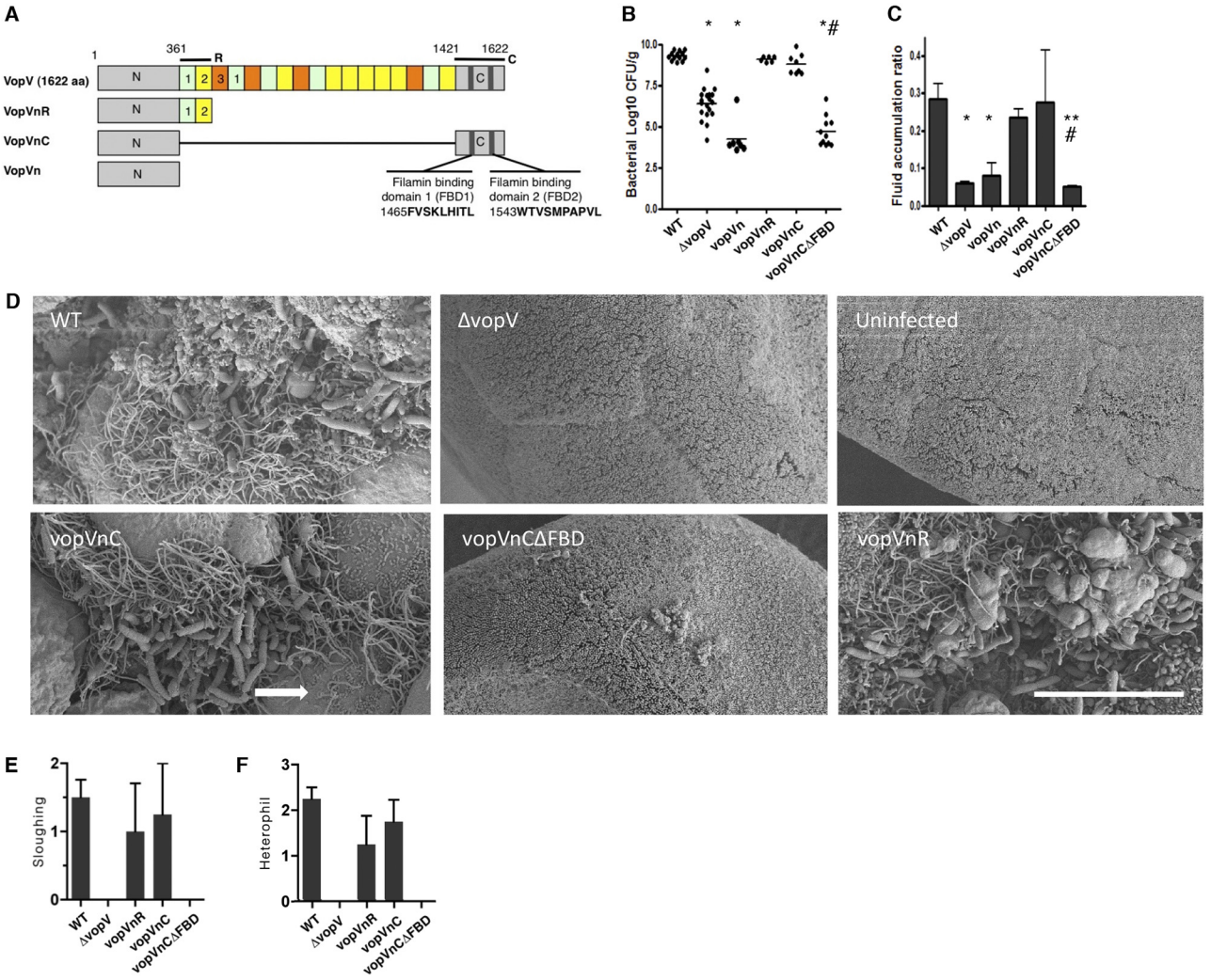

FIG 1 Schematic structure of VopV and the effects of various VopV mutants on *V. parahaemolyticus* virulence in infant rabbits. (A) VopV contains an N-terminal region that includes its secretion signal (N), interspersed repeat sequences (1 to 3), and a C-terminal region (C) with two filamin-binding domains (FBDs). Mutant forms of chromosome-encoded VopV (VopVnR, VopVnC, VopVn) are shown underneath. VopVnCΔFBD (not shown) is equivalent to VopVnC except that both FBDs have been deleted. The VopVR and VopVC protein fragments used in transfection and pulldown assays are indicated at the top (R and C, respectively). Colonization of infant rabbit intestines ($n \geq 6$ rabbits) (B) and fluid accumulation ($n \geq 6$) (C) at 38 h postinfection with the indicated *V. parahaemolyticus* strains. For panel B, data points represent individual rabbits, * is the statistically significant difference relative to wt ($P < 0.001$), and # is a *P* value of <0.001 relative to VopVnC. (C) Averages and standard deviations (SD) for rabbits in panel B; * ($P < 0.05$) and ** ($P < 0.01$) are differences relative to the wt strain, and # ($P < 0.05$) is relative to the VopVnC strain. (D) SEM of tissue from the small intestines of infected rabbits 28 h postinfection. Bar, 10 μM. Arrow points to a region clearly showing effacement of microvilli. Epithelial sloughing ($n = 4$) (E) and heterophil infiltration ($n = 4$) (F) at 38 h postinfection with the indicated *V. parahaemolyticus* strains. Hematoxylin and eosin (H&E)-stained tissue sections were graded by a pathologist. Data in panels B and C for wt rabbits were previously reported (2, 11). Statistical analysis was with one-way analysis of variance (ANOVA) and Bonferroni's multiple comparison posttest.

the microvilli's actin cores, we pretreated Caco-2_{BBe} monolayers with Jasplakinolide, a cell-permeable macrocyclic peptide that inhibits F-actin turnover and thereby stabilizes microvilli (15). Jasplakinolide pretreatment markedly reduced adhesion by all strains that normally adhere robustly to untreated monolayers (those expressing VopV, VopVnR, or VopVnC) (Fig. 2A and B). Furthermore, when bacteria of these 3 strains bound to pretreated cells, no BB effacement and microvillus elongation was evident in the associated Caco-2_{BBe} cells, suggesting that *V. parahaemolyticus*-induced BB remodeling requires actin depolymerization and that such remodeling is required for robust adherence (Fig. 2A, right). Notably, Jasplakinolide pretreatment did not affect the minimal adhesion of the Δ*vopV* or *vscN2* (T3SS2-deficient) strains (Fig. 2B); thus, the adherence of these strains is not dependent on actin-based cytoskeletal rearrangements. Interestingly, the bacteria that minimally adhered to Caco-2_{BBe} monolayers in the absence of microvillus restructuring were present as single cells, rather than the bacterial clusters observed on effaced tissue. It is possible that microvillus effacement also facilitates interbacterial contacts and that such contacts promote *V. parahaemolyticus* adhesion to the intestinal surface.

We also assessed the consequences of pretreating differentiated Caco-2_{BBe} monolayers with cytochalasin D, a small molecule that depolymerizes actin filaments and effaces microvilli (16), prior to infection. Cytochalasin pretreatment slightly decreased the adherence of the VopV+, VopVnR, and VopVnC strains, all of which

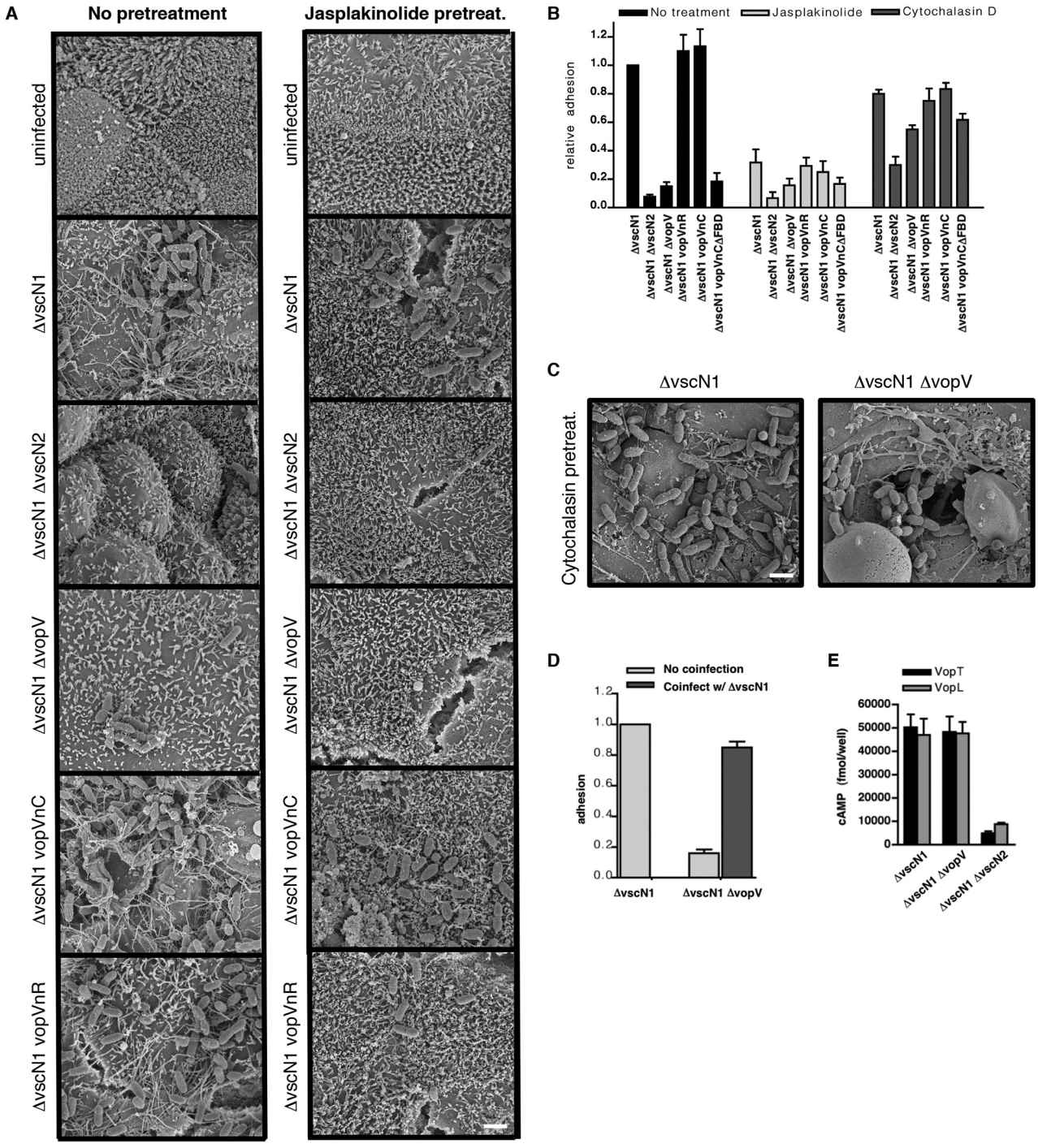

FIG 2 Comparative analyses of differentiated Caco-2_{BBe} monolayers infected with VopV mutants. All strains also contained mutations in *vscN1* to avoid the cytotoxic effects of T3SS1. Infected cells were pretreated with Jasplakinolide or cytochalasin D or left untreated. (A, C) Untreated and Jasplakinolide-treated cells (A) and cytochalasin-treated cells (C) were imaged using scanning electron microscopy. Scale bar, 2 μM. (B) Bacterial adhesion was quantified and normalized to the *vscN1* strain's adhesion to untreated cells (set to 1.0). (D) Adhesion of *vscN1 vopV* cells to differentiated Caco-2_{BBe} monolayers was enumerated both in the absence and presence of differentially marked *vscN1* cells. Adhesion was normalized to that of the *vscN1* strain alone. (E) Caco-2_{BBe} cells were infected with the indicated strains harboring plasmids encoding VopT-CyaA or VopL-CyaA, and effector translocation was assayed via measurement of intracellular cAMP. Mutant alleles of *vopV* are described in Fig. 1. Adhesion and translocation assays were performed in triplicate.

induce effacement of untreated Caco-2_{BBe} cells, but it markedly augmented the adherence of the typically nonadherent and non-effacing Δ*vopV* mutant (Fig. 2B and C). Furthermore, we found that a VopV+ strain could largely rescue the adherence of the Δ*vopV* mutant (to >80% of wt levels) when untreated Caco-2_{BBe} monolayers were coinfected with the two strains (Fig. 2D). Finally,

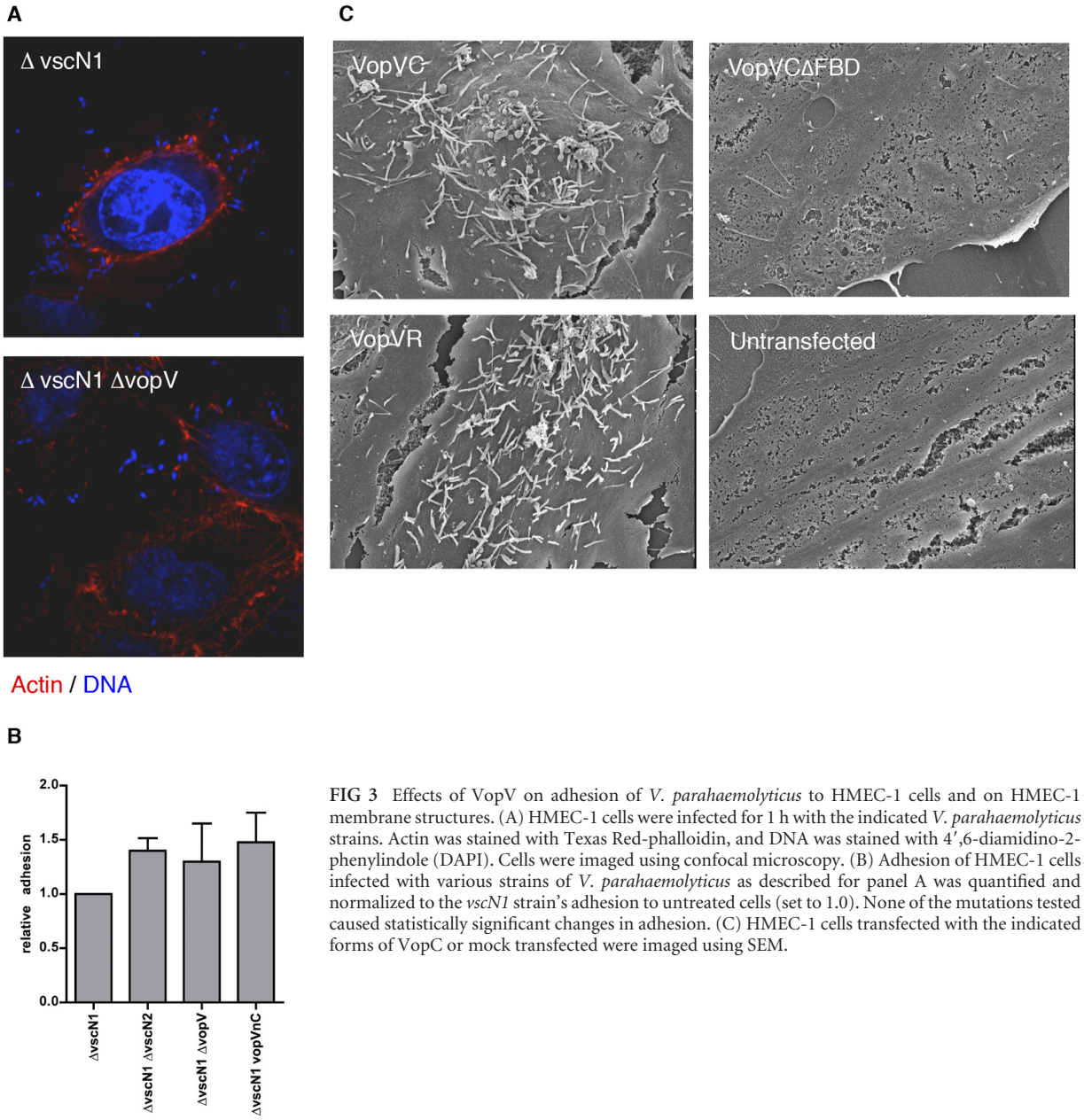

FIG 3 Effects of VopV on adhesion of *V. parahaemolyticus* to HMEC-1 cells and on HMEC-1 membrane structures. (A) HMEC-1 cells were infected for 1 h with the indicated *V. parahaemolyticus* strains. Actin was stained with Texas Red-phalloidin, and DNA was stained with 4′,6-diamidino-2-phenylindole (DAPI). Cells were imaged using confocal microscopy. (B) Adhesion of HMEC-1 cells infected with various strains of *V. parahaemolyticus* as described for panel A was quantified and normalized to the *vscN1* strain's adhesion to untreated cells (set to 1.0). None of the mutations tested caused statistically significant changes in adhesion. (C) HMEC-1 cells transfected with the indicated forms of VopC or mock transfected were imaged using SEM.

we found that deletion of *vopV* did not impair adhesion of *V. parahaemolyticus* to human microvascular epithelial cells (HMEC-1), which lack microvilli (Fig. 3A and B). These results all suggest that VopV's key role during colonization is to efface the BB membrane, which is a prerequisite for bacterial adhesion. VopV is not required for adhesion of *V. parahaemolyticus* to host cells, although it may enhance this process, potentially along with other T3SS2 proteins. Our data also suggest that the elongated microvilli that often surround attached *V. parahaemolyticus* are dispensable for bacterial adhesion, since extensive adhesion is evident in the presence of cytochalasin, which largely prevents formation of these actin-rich structures. VopV's role as a modulator of the brush border architecture highlights the importance of analyzing host-pathogen interactions using physiologically relevant model systems.

Due to the effect of VopV on bacterial association with host cells, we hypothesized that VopV might facilitate the transfer of other T3SS effectors. We therefore monitored the effect of VopV on translocation of T3SS2 effector-CyaA fusion proteins into differentiated Caco-2_{BBe} monolayers. Surprisingly, we found that deletion of an essential T3SS2 component (VscN2), but not deletion of VopV alone, markedly diminished translocation of the T3SS reporter molecules VopT-CyaA and VopL-CyaA (Fig. 2E). Thus, the reduced BB effacement associated with VopV-deficient strains appears to be a direct consequence of the absence of VopV alone. These data also suggest that relatively loose adhesion of *V. parahaemolyticus* to host cells is sufficient to enable translocation of T3SS2 effectors.

We explored the molecular basis of VopV's activity by using the full-length protein as bait in a yeast two-hybrid screen. Unex-

pectedly, this screen did not detect an interaction between VopV and actin; however, it yielded >30 distinct hits to filamins A, B, and C, which are members of a family of large actin-binding proteins that promote orthogonal actin branching (17) and were not previously known to bind VopV. The N-terminal region of filamin binds actin, while the remainder of the protein, which consists largely of 24 repeat units, has numerous interaction partners, including factors that modulate cell adhesion, receptors, channels, and intracellular signaling molecules (18). Affinity purification of VopV, followed by mass spectrometry-based identification of interacting proteins in eukaryotic cell lysates, confirmed that all 3 filamin isoforms interact with VopV. Additionally, it revealed that filamins bind the C-terminal 200 aa of VopV (VopVC) but not a subset of VopV's repeat sequences (repeats 1 and 2, henceforth termed VopVR) (Fig. 4A). In contrast, our copurification studies suggest that actin binds VopVR (as previously observed [13]) but not VopVC. It is not clear why our results regarding actin binding of the C terminus of VopV differ from those of a previous report (13). Finally, pulldown studies using purified His-tagged filamin A (FLNA) repeats 1 to 8, 8 to 15, and 16 to 24 revealed that VopVC directly binds protein fragments containing repeats 8 to 15 and 16 to 24 and that this binding is dependent upon two bioinformatically predicted filamin-binding domains (FBDs) (Fig. 1A and 4B, C, and D). The FBDs are also required for colocalization of filamin and VopVC in transfected HMEC-1 cells, which was investigated using immunofluorescence microscopy (Fig. 4D). Colocalization was explored in HMEC-1 cells because we were unable to transfect fully differentiated Caco-2_{BBe} cells.

Infection analyses, using both infant rabbits and differentiated Caco-2_{BBe} cells, revealed that VopV's FBDs are important for the effector's activity against host cells. When the FBDs were absent from VopV's C terminus (VopVnCΔFBD), *V. parahaemolyticus* could not colonize infant rabbits (Fig. 1B) and did not induce intestinal fluid accumulation or disrupt intestinal microvilli (Fig. 1C and D). A strain producing VopVnCΔFBD also displayed markedly reduced adhesion to differentiated Caco-2_{BBe} cells, comparable to that exhibited by the T3SS2- and VopV-deficient strains (Fig. 2B). Furthermore, immunostaining of infected Caco-2_{BBe} cells revealed that the FBDs contribute to the cytoskeletal alterations induced by infection with *V. parahaemolyticus*. Differentiated monolayers infected with a T3SS2-deficient strain or the VopVnCΔFBD strain or mock infected retained a uniform surface of actin-rich microvilli, and an FLNA-rich zone was often present immediately below. In contrast, actin in monolayers infected with adherent strains (VopV+, VopVnR, and VopVnC) was disorganized, and an underlying filamin layer was rarely evident (Fig. 5). These data provide additional evidence that VopV enables *V. parahaemolyticus* to remodel the host cell cytoskeleton via binding to filamin as well as to actin. Interactions between effectors and filamin have been observed for *Salmonella* and atypical *V. cholerae* but have not previously been shown to modulate BB dynamics (19, 20).

Finally, we used SEM to assess the consequences of VopV on the eukaryotic cell cytoskeleton in the absence of other T3SS2 proteins. For these experiments, VopVC, VopVR, and VopVCΔFBD were each transfected into HMEC-1 cells, which lack microvilli; consequently, we could investigate formation of elongated microvilli but not VopV's sufficiency to induce microvillus effacement. Notably, VopVC and VopVR both induced formation of elongated microvillus-like appendages reminiscent

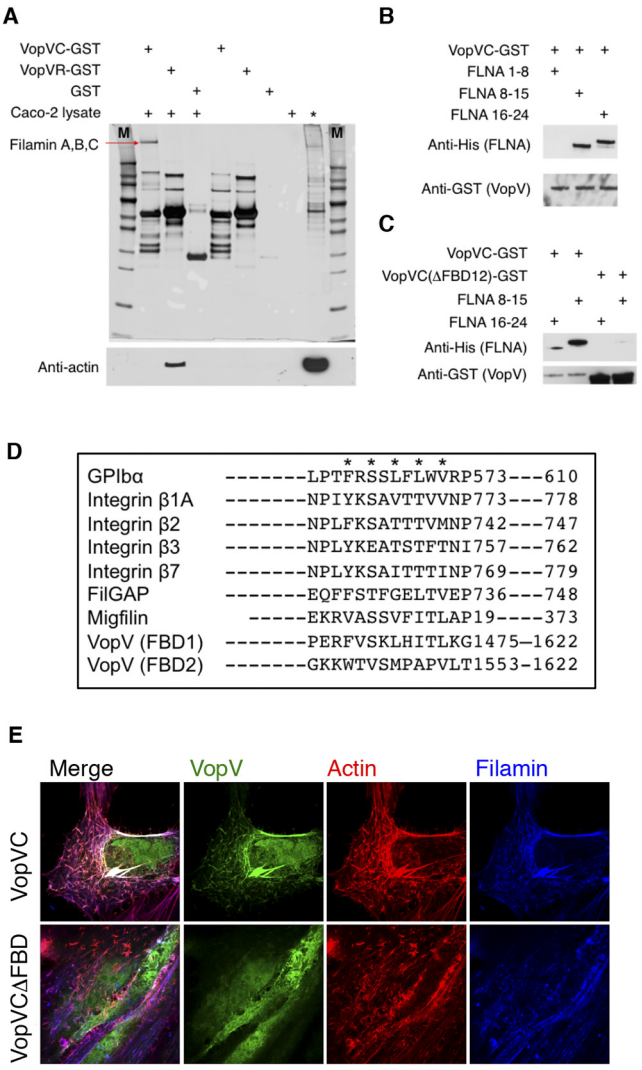

FIG 4 Mapping of VopV and filamin's interacting domains. (A, B, C) Affinity purification was performed on glutathione agarose columns, using GST-tagged fragments of VopV (defined in Fig. 1) and either Caco-2 cell lysates or His-tagged subsets of FLNA repeats. (A) Purified proteins were silver stained, and the band of interest (arrow) was analyzed by mass spectrometry (top) or analyzed by Western blotting (anti-actin; bottom). M denotes molecular weight markers and * shows unpurified Caco-2 lysate. (B, C) Purified proteins were detected via immunoblotting with anti-His and anti-GST. (D) The amino acid sequence alignment of predicted VopV filamin-binding domains 1 (FBD-1) and 2 and filamin-binding sites of human GPIbα, β-integrins, FilGAP, and migfilin. Amino acids indicated with asterisks face a groove generated between the C and D strands of the filamin immunoglobulin-like domain, which are involved mainly in binding interaction. (E) HMEC-1 cells transfected with the indicated forms of VopV (HA tagged) were labeled with anti-HA (green), anti-filamin (blue), and the actin stain Texas Red-phalloidin (red) and visualized using fluorescence microscopy.

of those seen *in vivo* and on differentiated Caco-2_{BBe} cells after *V. parahaemolyticus* infection. In contrast, VopVCΔFBD did not alter HMEC-1 surfaces; VopVCΔFBD-transfected cells, like untransfected cells, had smooth cell membranes (Fig. 3B). Thus, even in the absence of other T3SS2-secreted factors, VopV's actin and filamin-binding activities are each sufficient to induce actin-based remodeling of the host cell surface, likely by directly

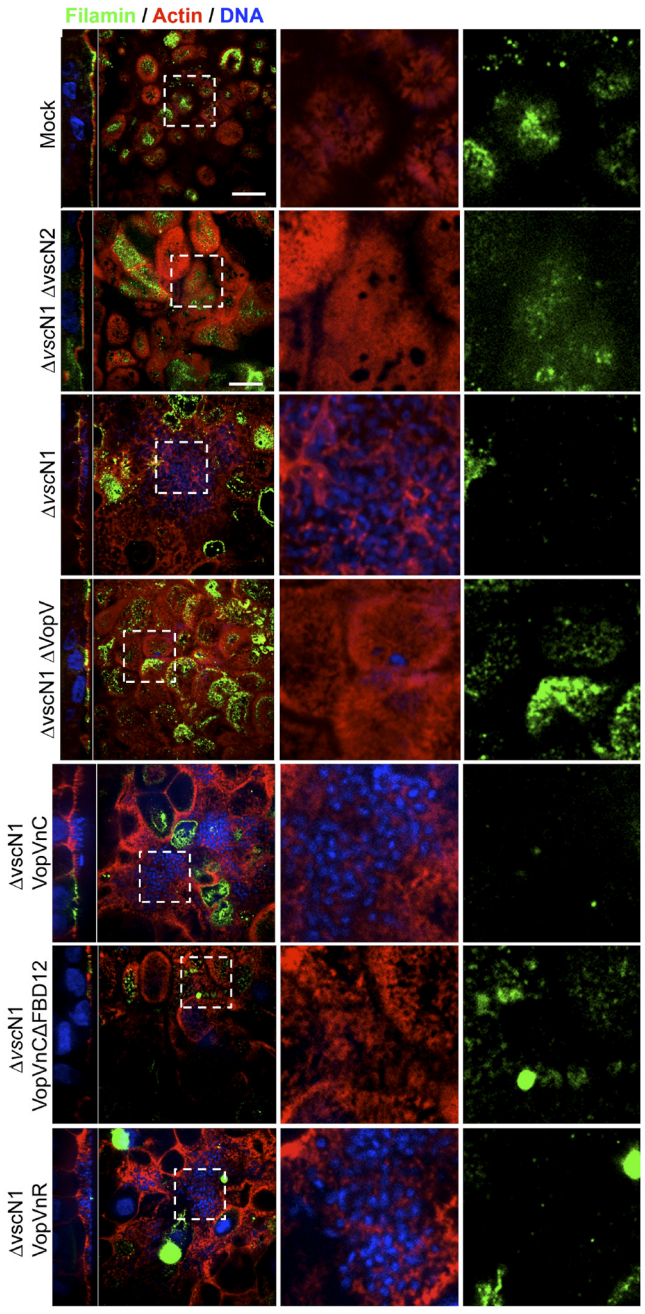

FIG 5 Infected Caco-2_{BBe} cells were stained with phalloidin (to detect actin; red), anti-filamin A (green), and DAPI (to detect Caco-2 and bacterial DNA; blue) and visualized using confocal microscopy. Views show the *xz* (left) and *xy* projection views (rest). For selected regions of the *xy* projection (stippled-line squares), actin and DNA (first cropped image) and filamin alone (last cropped image) are shown. Scale bar, 10 μm. Mutant alleles of *vopV* are described in the legend to Fig. 1. Strains also contained mutations in *vscN1* to avoid the cytotoxic effects of T3SS1.

(VopVR) or indirectly (via filamin; VopVC) altering actin dynamics.

In summary, we demonstrate that VopV is essential for *V. parahaemolyticus* to colonize the intestine and induce diarrhea and histopathological evidence of infection/disease. Differentiated Caco-2_{BBe} monolayers infected with *V. parahaemolyticus* likewise demonstrate VopV-dependent microvillus effacement and elongation. *V. parahaemolyticus* lacking VopV does not adhere to differentiated Caco-2_{BBe} cells, which likely underlies the mutant's marked attenuation *in vivo*. VopV does not appear to be critical as a direct mediator of adhesion; instead, our data suggest that VopV's primary activity is to promote BB rearrangement, through its binding to actin and filamin, and that the resulting effacement is a necessary precursor to bacterial adhesion and pathogenesis. Whether effacement merely provides an altered surface for adhesion, or exposes membrane domains and/or a specific host receptor that the pathogen does not have access to in the intact BB, remains to be determined. Additional studies to define *V. parahaemolyticus* factors that directly mediate bacterial adhesion are also warranted.

VopV's actin-binding repeats and its filamin-binding C terminus are functionally redundant, in that translocation of either by *V. parahaemolyticus* is sufficient for BB remodeling, enterocyte adherence, intestinal colonization, and virulence. By interacting with the highly networked protein filamin as well as actin, VopV likely provides *V. parahaemolyticus* with greater scope to modulate host cell processes linked to the actin cytoskeleton. The T3SS2 effectors VopL and VopC have also been reported to influence (either directly or indirectly) the actin-based cytoskeleton, although unlike VopV, these factors are not required for *V. parahaemolyticus* pathogenicity (10–12, 21). Determining if and how the activities of these 3 effectors are coordinated will be an interesting challenge for future research. Further studies of cytoskeletal rearrangement may also provide more understanding of the role of extended microvilli in *V. parahaemolyticus*-associated disease.

V. parahaemolyticus' remodeling of the enterocyte BB is reminiscent of, but not identical to, the effects of traditional attaching and effacing (A/E) pathogens, e.g., EHEC, EPEC, and *Citrobacter rodentium*, which all induce effacement of microvilli underneath host cell-associated bacteria (1, 22, 23). However, *V. parahaemolyticus*, unlike the A/E pathogens, does not induce formation of actin-rich pedestals in host cells, nor does it induce the extensive bacterium-host cell contact that A/E pathogens trigger via binding of the bacterial protein intimin and its translocated receptor, Tir. Instead, *V. parahaemolyticus* appears to form relatively limited contacts with host cells, and interbacterial contacts are more evident than with A/E pathogens. Our analyses also suggest that VopV plays a more pivotal role in effacement than any of the effacement-linked effectors in A/E pathogens (e.g., Map, EspF, Tir), which are collectively, rather than individually, required (24, 25). Notably, VopV has no homology to any of these other effectors, suggesting that the various species have independently evolved means to alter the host BB. At least *in vitro*, neither the absence of VopV nor of EPEC effacement-mediating effectors (25) reduces effector translocation overall, despite the marked effects of their absences on bacterial adhesion to host cells; thus, the phenotypes associated with these mutants can be attributed to the absence of specific effectors in host cells rather than a general translocation deficiency. *In vivo*, the failure of VopV-deficient *V. parahaemolyticus* to colonize the intestine, like that seen for EHEC with impaired effacement (e.g., *tir* mutants) (26), suggests that disruption of the enterocyte BB is a key step underlying attachment and pathogenicity of noninvasive T3SS-bearing enteric pathogens.

MATERIALS AND METHODS

Bacterial strains and plasmids. All strains are derived from RIMD2210633 (6). The *vscN1* and *vscN1 vscN2* strains have been described previously (9). Additional mutants, including *vopV*, *vopVnR*, *vopVnC*, and *vopVnCΔFBD* strains, were created as described in reference 27. Plasmid pVopL-CyaA was created by cloning the first 133 codons of VopL in frame with *cyaA* in pMMB207 (28), and pVopT-CyaA, a similar pMMB207 derivate, was described in reference 29. Expression constructs for glutathione *S*-transferase (GST)-tagged VopVR or VopVC were generated from pGEX4T1 (GE Healthcare). The expression constructs for His-tagged FLNA fragments are described in reference 30.

Rabbit infections. Infant rabbits were infected as previously described (2, 11). Briefly, ranitidine-treated rabbits were orogastrically inoculated with 10^9 CFU of *V. parahaemolyticus*, and bacterial colonization (CFU/g intestinal tissue), fluid accumulation, and histological changes were measured 38 h postinfection. Histological scoring was performed by a pathologist as described in reference 2. Samples for SEM of intestinal tissues were collected 28 h postinfection, as tissue architecture is too severely perturbed for analyses at later time points.

Ethics statement. This study was performed in strict accordance with the recommendations in the *Guide for the Care and Use of Laboratory Animals* of the National Institutes of Health (31). All animal protocols were reviewed and approved by the Harvard Medical Area Standing Committee on Animals (protocol number 04308).

Eukaryotic cell culture and infection. Caco-2_{BBe} cells were routinely maintained in Dulbecco's modified Eagle's medium (DMEM) with 15% fetal bovine serum (FBS). Differentiated Caco-2_{BBe} cell monolayers were prepared by plating trypsinized cells into 24-well transwells and growing for ~14 days (14). *V. parahaemolyticus* cells used to infect Caco-2_{BBe} cells were grown in LB with 0.04% sodium cholate for 2 h prior to infection, in order to induce the expression of T3SS2. All bacterial strains used for infection of Caco-2_{BBe} cells lacked functional T3SS1 (due to Δ*vscN1*), in order to avoid the cytotoxicity associated with T3SS1 *in vitro*. Differentiated Caco-2_{BBe} monolayers were infected with 10 μl of bacterial culture (~10^8 CFU) for 1.5 h in the presence of 0.04% sodium cholate. Measurement of bacterial adhesion to Caco-2_{BBe} monolayers and confocal microscopy analyses are described below. Additionally, infected cells were fixed and processed for SEM. Briefly, after infection, the polycarbonate membrane on which the differentiated cells were grown was excised from the transwell and immediately fixed with fixative containing picric acid and glutaraldehyde. SEM images were captured as previously described (2).

HMEC-1 cells were routinely maintained as previously described (32) and infected using the conditions described above for Caco-2_{BBe} cells. HMEC-1 cells were transfected with pCMV plasmids encoding VopVC, VopVR, or VopVCΔFBD for 24 h. Transfected cells were fixed and processed for SEM analysis.

Adhesion assays. Differentiated Caco-2_{BBe} cells were left untreated, pretreated with Jasplakinolide (0.5 μM; Santa Cruz Biotech) for 2 h, or pretreated with cytochalasin D (0.5 μg/ml; Sigma) for 10 h and then infected with *V. parahaemolyticus* for 1.5 h as described above. Infected Caco-2_{BBe} monolayers were washed with phosphate-buffered saline (PBS) 5 times to remove nonadherent bacteria, and subsequently the number of adherent bacterial CFU was determined via plating. For each experiment, the frequency of adhesion by the Δ*vscN1* strain was set to 1, and all other frequencies were calculated relative to this control strain. For coinfection, Caco-2_{BBe} monolayers were infected with 10 μl of a Δ*vscN1* Δ*vopV* strain harboring chloramphenicol resistance and 10 μl of the Δ*vscN1* mutant and compared to cells infected with each strain singly. The frequency of adherent chloramphenicol-resistant CFU was enumerated as described above for single infections and coinfections and compared to the frequency of adherent Δ*vscN1* bacteria.

Adhesion to HMEC-1 cells was performed similarly, except that cells were infected for 1 h.

Immunofluorescence labeling. Infected cells were extensively washed with PBS++ (supplemented with 1 mM $CaCl_2$ and 0.1 mM $MgCl_2$) and fixed with 4% paraformaldehyde (PFA) for 20 to 30 min at room temperature. Samples were permeabilized, quenched, and blocked with PBS++-50 mM NH_4Cl-5% bovine serum albumin (BSA)-0.1 g% Saponin for 10 min at room temperature. Filamin was detected with a rabbit polyclonal antibody raised against recombinant human FLNA repeat 1 (Pacific Immunology Corp.) and affinity purified using the repeat 1 protein immobilized on *N*-hydroxysuccinimide (NHS)-Sepharose beads. The purified antibodies, which were confirmed to specifically recognize FLNA, were then visualized with Alexa 488-labeled goat anti-rabbit secondary antibodies (Invitrogen). Actin was visualized using Texas Red-phalloidin (Invitrogen). Samples were mounted using Mowiol.

Confocal image acquisition, processing, and analysis Confocal images were acquired using a spinning disk confocal head (CSU-X1; PerkinElmer Co., Boston, MA) coupled to a fully motorized inverted Zeiss Axiovert 200-M microscope equipped with a ×63 magnification lens (Pan Apochromat; 1.4 numerical aperture [NA]) and with a 175-W xenon lamp Lambda DG-4 (Sutter Instruments, Novato, CA) for wide-field illumination. Solid-state lasers (473 nm, 568 nm, and 660 nm; Crystal Laser, Reno, NV) coupled to the spinning head through a fiber optic were used as a light source. An acoustic-optical tunable filter (AOTF) was used to switch between different wavelengths. The imaging system operates under control of SlideBook 5 (Intelligent Imaging Innovations Inc., Denver, CO) and includes a computer-controlled spherical aberration correction device (SAC; Intelligent Imaging Innovations, Inc., Denver, CO) installed between the objective lens and the charge-coupled-device (CCD) camera (QuantEM:512SC; Photometrics). Acquisition of sequential optical sections spaced 0.15 μm apart was achieved with the aid of a Piezoelectric Z motorized stage (ASI). Representative confocal images were selected and processed to make figures using Adobe Photoshop software.

Effector-CyaA fusion protein-based analysis of effector translocation. Caco-2_{BBe} cells were cultured for 14 days to achieve differentiation and then infected for 1.5 h in the presence of 0.04% sodium cholate with *vscN1*, *vscN1 vopV*, and *vscN1 vscN2* strains containing pVopT-CyaA or pVopL-CyaA. Subsequently, cyclic AMP (cAMP) levels were determined by enzyme-linked immunosorbent assay (ELISA) as described (29).

Yeast two-hybrid and pulldown assay. Yeast two-hybrid analysis was performed by Hybrigenics (France). Briefly, full-length *vopV* was used to screen a placental cDNA library. Clones expressing proteins with positive interactions with VopV were isolated and sequenced, and all clones with high confidence interactions were found to express isoforms of filamin. The interaction between VopV and filamin was confirmed via copurification using GST-tagged VopV fragments and Caco-2 lysates. Briefly, whole-cell lysates of *E. coli* BL21 overexpressing GST-tagged VopVC, GST-tagged VopVR, or GST alone were loaded onto spin columns containing 100 μl glutathione agarose and incubated for 1 to 2 h. The agarose was thoroughly washed with PBS 5 to 7 times before being mixed with whole-cell lysates of Caco-2 cells. After 1 h of incubation, the agarose was further washed 5 to 7 times with PBS and eluted with glutathione (10 mM). Eluted fractions were separated by SDS-polyacrylamide gel electrophoresis. A protein band detected only in the eluate containing VopVC-GST was analyzed by mass spectrometry (Taplin Mass Spectrometry Facility, Harvard Medical School) and found to contain filamins A, B, and C. Column eluates were also analyzed by Western blotting using an antiactin antibody. Additional copurification analyses were performed using GST-tagged VopVR and VopVC and derivatives lacking one (VopVCΔFBD1) or both (VopVCΔFBD12) FBDs, which were incubated with His-tagged filamin fragments (30) for 1 h. Eluates from glutathione agarose columns were analyzed using Western blotting with anti-His and anti-GST antibodies.

ACKNOWLEDGMENTS

X.Z. was supported by an NERCE Fellowship (U54 AI 057159). F.N. was supported by NIH grant number HL19749. B.E.G. was supported by NIH grant K08 CA140780 and a Burroughs Wellcome Medical Scientist Career Award. W.I.L. was supported by NIH grants DK48106 and DK84424 and

HDDC grant P30 DK34854. M.K.W. was supported by NIH grant R37 AI042347 and HHMI.

We are grateful to Rod Bronson for assistance with analysis of tissue sections and Marian Neutra and John Mekalanos for insightful comments on the manuscript.

REFERENCES

1. **Wong AR, Pearson JS, Bright MD, Munera D, Robinson KS, Lee SF, Frankel G, Hartland EL.** 2011. Enteropathogenic and enterohaemorrhagic *Escherichia coli*: even more subversive elements. Mol. Microbiol. **80:**1420–1438. http://dx.doi.org/10.1111/j.1365-2958.2011.07661.x.
2. **Ritchie JM, Rui H, Zhou X, Iida T, Kodoma T, Ito S, Davis BM, Bronson RT, Waldor MK.** 2012. Inflammation and disintegration of intestinal villi in an experimental model for *Vibrio parahaemolyticus*-induced diarrhea. PLoS Pathog. **8:**e1002593. http://dx.doi.org/10.1371/journal.ppat.1002593.
3. **Qadri F, Alam MS, Nishibuchi M, Rahman T, Alam NH, Chisti J, Kondo S, Sugiyama J, Bhuiyan NA, Mathan MM, Sack DA, Nair GB.** 2003. Adaptive and inflammatory immune responses in patients infected with strains of *Vibrio parahaemolyticus*. J. Infect. Dis. **187:**1085–1096. http://dx.doi.org/10.1086/368257.
4. **Galán JE.** 2009. Common themes in the design and function of bacterial effectors. Cell Host Microbe **5:**571–579. http://dx.doi.org/10.1016/j.chom.2009.04.008.
5. **Dean P.** 2011. Functional domains and motifs of bacterial type III effector proteins and their roles in infection. FEMS Microbiol. Rev. **35:**1100–1125. http://dx.doi.org/10.1111/j.1574-6976.2011.00271.x.
6. **Makino K, Oshima K, Kurokawa K, Yokoyama K, Uda T, Tagomori K, Iijima Y, Najima M, Nakano M, Yamashita A, Kubota Y, Kimura S, Yasunaga T, Honda T, Shinagawa H, Hattori M, Iida T.** 2003. Genome sequence of *Vibrio parahaemolyticus*: a pathogenic mechanism distinct from that of *V. cholerae*. Lancet **361:**743–749. http://dx.doi.org/10.1016/S0140-6736(03)12659-1.
7. **Broberg CA, Calder TJ, Orth K.** 2011. *Vibrio parahaemolyticus* cell biology and pathogenicity determinants. Microbes Infect. **13:**992–1001. http://dx.doi.org/10.1016/j.micinf.2011.06.013.
8. **Park KS, Ono T, Rokuda M, Jang MH, Okada K, Iida T, Honda T.** 2004. Functional characterization of two type III secretion systems of *Vibrio parahaemolyticus*. Infect. Immun. **72:**6659–6665. http://dx.doi.org/10.1128/IAI.72.11.6659-6665.2004.
9. **Hiyoshi H, Kodama T, Iida T, Honda T.** 2010. Contribution of *Vibrio parahaemolyticus* virulence factors to cytotoxicity, enterotoxicity, and lethality in mice. Infect. Immun. **78:**1772–1780. http://dx.doi.org/10.1128/IAI.01051-09.
10. **Liverman AD, Cheng HC, Trosky JE, Leung DW, Yarbrough ML, Burdette DL, Rosen MK, Orth K.** 2007. Arp2/3-independent assembly of actin by *Vibrio* type III effector VopL. Proc. Natl. Acad. Sci. U. S. A. **104:**17117–17122. http://dx.doi.org/10.1073/pnas.0703196104.
11. **Zhou X, Gewurz BE, Ritchie JM, Takasaki K, Greenfeld H, Kieff E, Davis BM, Waldor MK.** 2013. A *Vibrio parahaemolyticus* T3SS effector mediates pathogenesis by independently enabling intestinal colonization and inhibiting TAK1 activation. Cell. Rep. **3:**1690–1702. http://dx.doi.org/10.1016/j.celrep.2013.03.039.
12. **Okada R, Zhou X, Hiyoshi H, Matsuda S, Chen X, Akeda Y, Kashimoto T, Davis BM, Iida T, Waldor MK, Kodama T.** 2014. The *Vibrio parahaemolyticus* effector VopC mediates Cdc42-dependent invasion of cultured cells but is not required for pathogenicity in an animal model of infection. Cell. Microbiol. **16:**938–947. http://dx.doi.org/10.1111/cmi.12252.
13. **Hiyoshi H, Kodama T, Saito K, Gotoh K, Matsuda S, Akeda Y, Honda T, Iida T.** 2011. VopV, an F-actin-binding type III secretion effector, is required for *Vibrio parahaemolyticus*-induced enterotoxicity. Cell Host Microbe **10:**401–409. http://dx.doi.org/10.1016/j.chom.2011.08.014.
14. **Peterson MD, Mooseker MS.** 1993. An *in vitro* model for the analysis of intestinal brush border assembly. I. Ultrastructural analysis of cell contact-induced brush border assembly in Caco-2BBe cells. J. Cell Sci. **105:**445–460.
15. **Bubb MR, Senderowicz AM, Sausville EA, Duncan KL, Korn ED.** 1994. Jasplakinolide, a cytotoxic natural product, induces actin polymerization and competitively inhibits the binding of phalloidin to F-actin. J. Biol. Chem. **269:**14869–14871.
16. **Cooper JA.** 1987. Effects of cytochalasin and phalloidin on actin. J. Cell Biol. **105:**1473–1478. http://dx.doi.org/10.1083/jcb.105.4.1473.
17. **Stossel TP, Condeelis J, Cooley L, Hartwig JH, Noegel A, Schleicher M, Shapiro SS.** 2001. Filamins as integrators of cell mechanics and signalling. Nat. Rev. Mol. Cell Biol. **2:**138–145. http://dx.doi.org/10.1038/35052082.
18. **Nakamura F, Stossel TP, Hartwig JH.** 2011. The filamins: organizers of cell structure and function. Cell Adh. Migr. **5:**160–169. http://dx.doi.org/10.4161/cam.5.2.14401.
19. **Miao EA, Brittnacher M, Haraga A, Jeng RL, Welch MD, Miller SI.** 2003. *Salmonella* effectors translocated across the vacuolar membrane interact with the actin cytoskeleton. Mol. Microbiol. **48:**401–415. http://dx.doi.org/10.1046/j.1365-2958.2003.t01-1-03456.x.
20. **Tam VC, Suzuki M, Coughlin M, Saslowsky D, Biswas K, Lencer WI, Faruque SM, Mekalanos JJ.** 2010. Functional analysis of VopF activity required for colonization in *Vibrio cholerae*. mBio **1**(5):e00289-10. http://dx.doi.org/10.1128/mBio.00289-10.
21. **Zhang L, Krachler AM, Broberg CA, Li Y, Mirzaei H, Gilpin CJ, Orth K.** 2012. Type III effector VopC mediates invasion for *Vibrio* species. Cell. Rep. **1:**453–460. http://dx.doi.org/10.1016/j.celrep.2012.04.004.
22. **Deng W, Vallance BA, Li Y, Puente JL, Finlay BB.** 2003. *Citrobacter rodentium* translocated intimin receptor (Tir) is an essential virulence factor needed for actin condensation, intestinal colonization and colonic hyperplasia in mice. Mol. Microbiol. **48:**95–115. http://dx.doi.org/10.1046/j.1365-2958.2003.03429.x.
23. **Lai Y, Rosenshine I, Leong JM, Frankel G.** 2013. Intimate host attachment: enteropathogenic and enterohaemorrhagic *Escherichia coli*. Cell. Microbiol. **15:**1796–1808. http://dx.doi.org/10.1111/cmi.12179.
24. **Shaw RK, Cleary J, Murphy MS, Frankel G, Knutton S.** 2005. Interaction of enteropathogenic *Escherichia coli* with human intestinal mucosa: role of effector proteins in brush border remodeling and formation of attaching and effacing lesions. Infect. Immun. **73:**1243–1251. http://dx.doi.org/10.1128/IAI.73.2.1243-1251.2005.
25. **Dean P, Maresca M, Schüller S, Phillips AD, Kenny B.** 2006. Potent diarrheagenic mechanism mediated by the cooperative action of three enteropathogenic *Escherichia coli*-injected effector proteins. Proc. Natl. Acad. Sci. U. S. A. **103:**1876–1881. http://dx.doi.org/10.1073/pnas.0509451103.
26. **Ritchie JM, Thorpe CM, Rogers AB, Waldor MK.** 2003. Critical roles for *stx2*, *eae*, and *tir* in enterohemorrhagic *Escherichia coli*-induced diarrhea and intestinal inflammation in infant rabbits. Infect. Immun. **71:**7129–7139. http://dx.doi.org/10.1128/IAI.71.12.7129-7139.2003.
27. **Zhou X, Shah DH, Konkel ME, Call DR.** 2008. Type III secretion system 1 genes in *Vibrio parahaemolyticus* are positively regulated by ExsA and negatively regulated by ExsD. Mol. Microbiol. **69:**747–764. http://dx.doi.org/10.1111/j.1365-2958.2008.06326.x.
28. **Morales VM, Bäckman A, Bagdasarian M.** 1991. A series of wide-host-range low-copy-number vectors that allow direct screening for recombinants. Gene **97:**39–47. http://dx.doi.org/10.1016/0378-1119(91)90007-X.
29. **Zhou X, Ritchie JM, Hiyoshi H, Iida T, Davis BM, Waldor MK, Kodama T.** 2012. The hydrophilic translocator for *Vibrio parahaemolyticus*, T3SS2, is also translocated. Infect. Immun. **80:**2940–2947. http://dx.doi.org/10.1128/IAI.00402-12.
30. **Playford MP, Nurminen E, Pentikäinen OT, Milgram SL, Hartwig JH, Stossel TP, Nakamura F.** 2010. Cystic fibrosis transmembrane conductance regulator interacts with multiple immunoglobulin domains of filamin A. J. Biol. Chem. **285:**17156–17165. http://dx.doi.org/10.1074/jbc.M109.080523.
31. **National Research Council.** 2011. Guide for the care and use of laboratory animals, 8th ed. National Academies Press, Washington, DC.
32. **Weflen AW, Baier N, Tang QJ, Van den Hof M, Blumberg RS, Lencer WI, Massol RH.** 2013. Multivalent immune complexes divert FcRn to lysosomes by exclusion from recycling sorting tubules. Mol. Biol. Cell **24:**2398–2405. http://dx.doi.org/10.1091/mbc.E13-04-0174.